



HAL
open science

Distinct antibody responses to SARS-CoV-2 in children and adults across the COVID-19 clinical spectrum

Stuart Weisberg, Thomas Connors, Yun Zhu, Matthew Baldwin, Wen-Hsuan Lin, Sandeep Wontakal, Peter Szabo, Steven Wells, Pranay Dogra, Joshua Gray, et al.

► **To cite this version:**

Stuart Weisberg, Thomas Connors, Yun Zhu, Matthew Baldwin, Wen-Hsuan Lin, et al.. Distinct antibody responses to SARS-CoV-2 in children and adults across the COVID-19 clinical spectrum. Nature Immunology, 2020, pp.25-31. 10.1038/s41590-020-00826-9 . hal-03008774

HAL Id: hal-03008774

<https://cnrs.hal.science/hal-03008774>

Submitted on 17 Nov 2021

HAL is a multi-disciplinary open access archive for the deposit and dissemination of scientific research documents, whether they are published or not. The documents may come from teaching and research institutions in France or abroad, or from public or private research centers.

L'archive ouverte pluridisciplinaire **HAL**, est destinée au dépôt et à la diffusion de documents scientifiques de niveau recherche, publiés ou non, émanant des établissements d'enseignement et de recherche français ou étrangers, des laboratoires publics ou privés.

Figure #	Figure title One sentence only	Filename This should be the name the file is saved as when it is uploaded to our system. Please include the file extension. i.e.: <i>Smith_ED_Fig1.jpg</i>	Figure Legend If you are citing a reference for the first time in these legends, please include all new references in the Online Methods References section, and carry on the numbering from the main References section of the paper.
Extended Data Fig. 1	Specificity of subjects' antibodies for SARS-CoV-2 S protein.	extended_data_1.eps	<p>The specificity of antibodies for SARS-CoV-2 S protein compared to SARS-CoV-1 and MERS S protein was assayed in a cell-based IgG binding assay. HEK293T cells were transfected with S protein and its common variants from the indicated coronaviruses. The transfected cells were then incubated with human plasma from the indicated study groups and bound human IgG was detected using fluorescently tagged protein G (see methods). Shown are the percentage of the S protein transfected cells that are positive for human IgG in each patient group: CPD, black squares, n=19; COVID-ARDS, red squares, n=13; pediatric non-MIS-C, n=28; MIS-C, green circles, n=16; and control plasma from pre-pandemic donors (grey triangles; Neg, n=6). Black bar indicates the median+interquartile range. P values were calculated by one-way ANOVA with Dunnett's multiple comparisons test (CPD, SARS-CoV-2 vs. SARS-CoV-1: P=0, SARS-CoV-2 vs. MERS: P=0; COVID-ARDS, SARS-CoV-2 vs. SARS-CoV-1: P=0, SARS-CoV-2 vs. MERS: P=0; Ped non-MIS-C, SARS-CoV-2 vs. SARS-</p>

			CoV-1: P=0, SARS-CoV-2 vs. MERS: P=0; MIS-C, SARS-CoV-2 vs. SARS-CoV-1: P=0, SARS-CoV-2 vs. MERS: P=0; Negative control, SARS-CoV-2 vs. SARS-CoV-1: P=0.32, SARS-CoV-2 vs. MERS: P=0.52).
--	--	--	---

1

Item	Present?	Filename This should be the name the file is saved as when it is uploaded to our system, and should include the file extension. The extension must be .pdf	A brief, numerical description of file contents. i.e.: <i>Supplementary Figures 1-4, Supplementary Discussion, and Supplementary Tables 1-4.</i>
Supplementary Information	Yes	Supp-tables.pdf	Supplementary Tables 1-3
Reporting Summary	Yes	nr-reporting-NI-LE30732A	
Peer Review Information	Yes	<i>OFFICE USE ONLY</i>	

2

Figure	Filename This should be the name the file is saved as when it is uploaded to our system, and should include the file extension. i.e.: <i>Smith_SourceData_Fig1.xls</i> , or <i>Smith_Unmodified_Gels_Fig1.pdf</i>	Data description i.e.: Unprocessed Western Blots and/or gels, Statistical Source Data, etc.
Source Data Fig. 1	SOURCE_DATA-Fig-1.xlsx	Statistical Source Data
Source Data Fig. 2	SOURCE_DATA-Fig-2.xlsx	Statistical Source Data
Source Data Fig. 3	SOURCE_DATA-Fig-3.xlsx	Statistical Source Data
Source Data Fig. 4	SOURCE_DATA-Fig-4.xlsx	Statistical Source Data
Source Data Extended Data Fig. 1	SOURCE_DATA-Ex-Fig-1.xlsx	Statistical Source Data

3

4

5

6 **Distinct antibody responses to SARS-CoV-2 in children and adults across the COVID-19 clinical spectrum**

7

8

9

10 Stuart P. Weisberg^{1†}, Thomas J. Connors^{2†}, Yun Zhu^{2,3}, Matthew R. Baldwin⁴, Wen-hsuan Lin¹, Sandeep Wontakal¹, Peter A.
11 Szabo⁵, Steven B. Wells⁶, Pranay Dogra⁵, Joshua Gray⁵, Emma Idzikowski², Debora Stelitano^{2,3,7}, Francesca T. Bovier^{2,3,7},
12 Julia Davis-Porada⁸, Rei Matsumoto^{5,9}, Maya Meimei Li Poon⁵, Michael Chait^{1,5}, Cyrille Mathieu¹⁰, Branka Horvat¹⁰, Didier
13 Decimo¹⁰, Krystalyn E. Hudson¹, Flavia Dei Zotti¹, Zachary C. Bitan¹, Francesca La Carpia¹, Stephen A. Ferrara¹³, Emily
14 Mace², Joshua Milner², Anne Moscona^{2,3,11,12}, Eldad Hod¹, Matteo Porotto^{2,3,7*} and Donna L. Farber^{5,9,11*}

15

16 ¹Department of Pathology and Cell Biology, Columbia University Irving Medical Center, New York, NY 10032

17 ² Department of Pediatrics, Columbia University Irving Medical Center, New York, NY 10032

18 ³Center for Host-Pathogen Interactions, Columbia University Irving Medical Center, New York, USA

19 ⁴Department of Medicine, Columbia University Irving Medical Center, New York, NY 10032

20 ⁵Columbia Center for Translational Immunology, Columbia University Irving Medical Center, New York, NY 10032

21 ⁶Department of Systems Biology, Columbia University Irving Medical Center, New York, NY 10032

22 ⁷Department of Experimental Medicine, University of Study of Campania 'Luigi Vanvitelli', Naples, Italy

23 ⁸ Medical Scientist Training Program, Columbia University, New York, NY 10032

24 ⁹ Department of Surgery, Columbia University Irving Medical Center, New York, NY 10032

25 ¹⁰ CIRI, International Center for Infectiology Research, Inserm, U1111, University Claude Bernard Lyon 1, CNRS, UMR5308,

26 Ecole Normale Supérieure de Lyon, France

27 ¹¹ Department of Microbiology and Immunology, Columbia University Irving Medical Center, New York, NY 10032

28 ¹² Department of Physiology & Cellular Biophysics, Columbia University Irving Medical Center, New York, NY 10032

29 ¹³School of Nursing, Columbia University Irving Medical Center, New York, NY 10032

30 †co-first author

31 *co-senior author

32

33 Correspondence: Donna L. Farber, df2396@cumc.columbia.edu and Matteo Porotto, mp3509@cumc.columbia.edu

34 **INTRODUCTION**

35

36 Clinical manifestations of COVID-19 caused by the novel coronavirus SARS-CoV-2 are associated with age^{1,2}. Adults develop
37 respiratory symptoms, which can progress to Acute Respiratory Distress Syndrome (ARDS) in its most severe form, while children are
38 largely spared from respiratory illness but can develop a life-threatening multisystem inflammatory syndrome (MIS-C)³⁻⁵. Here, we
39 show distinct antibody responses in children and adults following SARS-CoV-2 infection. Adult COVID-19 cohorts had anti-Spike
40 (S) IgG, IgM and IgA antibodies, as well as anti-Nucleocapsid (N) IgG antibody, while children with and without MIS-C had reduced
41 breadth of anti-SARS-CoV-2-specific antibodies, predominantly generating IgG antibodies specific for the S protein but not for the N
42 protein. Moreover, children with and without MIS-C had reduced neutralizing activity compared to both adult COVID-19 cohorts,
43 indicating a reduced protective serological response. These results suggest a distinct infection course and immune response in children
44 independent of whether they develop MIS-C, with implications for developing age-targeted strategies for testing and protecting the
45 population.

46 **Main text**

47 The clinical manifestations of SARS-CoV-2 infection in children are distinct from adults. Children with COVID-19 rarely
48 exhibit severe respiratory symptoms and often remain asymptomatic², whereas adults experience respiratory symptoms of varying
49 severity, and older adults and those with co-morbidities such as hypertension and diabetes have significantly higher risks of
50 developing COVID-19-associated ARDS with high mortality^{2,6}. In children, a rare but severe clinical manifestation of SARS-CoV-2
51 infection designated Multisystem Inflammatory Syndrome in Children (MIS-C), exhibits similarities to Kawasaki disease in certain
52 inflammatory features and cardiovascular involvement while generally lacking severe respiratory symptoms³⁻⁵. The nature of the
53 immune response to SARS-CoV-2 in children with different clinical manifestations ranging from asymptomatic to MIS-C relative to
54 the more common respiratory manifestations of COVID-19 in adults, remains unclear.

55 The generation of virus-specific antibodies which neutralize or block infectivity is the most consistent correlate of protective
56 immunity for multiple infections and vaccines^{7,8}. Antibodies specific for the major SARS-CoV-2 antigens, including the Spike (S)
57 protein which binds the cellular receptor for viral entry, and the nucleocapsid (N) protein necessary for viral replication have been
58 detected in actively infected patients and in patients with mild disease who recovered⁹⁻¹². Anti-S antibodies, in particular, can exhibit
59 potent neutralizing activity and are currently being pursued as a therapeutic option for infusion into patients during severe disease and
60 for targeted generation in vaccines¹³⁻¹⁵. Defining the nature of the antibody response to SARS-CoV-2 infection as a function of age
61 and clinical syndrome can provide essential insights for improved screening and targeted protection for the global population that
62 continues to suffer from this relentless pandemic.

63 In this study, we investigated the specificity and functionality of the antibody response and its protective capacity in adult and
64 pediatric patients seen at Columbia University Irving Medical Center/New York-Presbyterian (CUIMC/NYP) hospital and the Morgan
65 Stanley Children's Hospital of New York (MSCHONY) during the height of the pandemic in New York City from March-June, 2020
66 ^{3,13,16,17}. We present 4 patient cohorts comprising a total of 79 individuals, including adults recruited as convalescent plasma donors
67 who recovered from mild COVID-19 respiratory disease without requiring hospitalization (CPD, n=19), adults hospitalized with
68 severe COVID-19 Acute Respiratory Distress Syndrome (COVID-ARDS, n=13), and two pediatric cohorts including children
69 hospitalized with MIS-C (MIS-C, n=16) and children who were infected with SARS-CoV-2 but did not develop MIS-C (Pediatric

70 Non-MIS-C, n=31) (See Table 1 for clinical characteristics). The adult cohorts represented a broad age range (19-84 y) while the
71 pediatric subjects were younger (3-18 y) (Table 1). Subjects were diagnosed as infected with SARS-CoV-2 based on history of
72 symptoms, PCR-positive test for virus and/or by serology (Table 1). While co-morbidities were rare among pediatric subjects, they
73 were frequently present in adult subjects with COVID-ARDS (Supplementary Table 1). Samples from COVID-ARDS and MIS-C
74 patients were obtained within 24-36 h of being admitted or intubated for respiratory failure, largely prior to the initiation of therapeutic
75 interventions (Supplementary Table 1). Samples from pediatric Non-MIS-C subjects were obtained during phlebotomy for various
76 clinical reasons, including routine screening for hospital admission and medical procedures (Supplementary Table 2), with 48%
77 having experienced no COVID-like symptoms and designated as asymptomatic. Both MIS-C and COVID-ARDS subjects exhibited
78 markers of systemic inflammation including highly elevated concentrations of interleukin 6 (IL-6) and C-reactive protein (CRP),
79 while ferritin and lactate dehydrogenase (LDH), were significantly increased in COVID-ARDS compared to MIS-C subjects (Table
80 1). Only 2 pediatric subjects developed respiratory failure and ARDS (Table 1; 1 with MIS-C and 1 non-MIS-C), indicating distinct
81 inflammatory responses and clinical manifestations between children and adults in response to infection.

82 We quantitated SARS-CoV-2 specific antibodies for each cohort in terms of specificity and antibody class, including IgM
83 generated initially in a primary response and IgG and IgA classes prominent in serum and secretions, respectively. Anti-S antibodies
84 were present as IgG (Fig. 1a), IgM (Fig. 1b) and IgA (Fig. 1c) classes in adult COVID-ARDS and CPD donors, with significantly
85 higher concentration in COVID-ARDS patients for all classes (Fig. 1a-c). By contrast, anti-S antibody titers and isotype predominance
86 in both pediatric cohorts (MIS-C and non-MIS-C) were similar to each other and to the adult CPD subjects—showing predominant
87 anti-S IgG (Fig. 1a), low titers of anti-S IgM (Fig. 1b) (similar to negative control pre-pandemic plasma), and variable titers of anti-S
88 IgA antibodies (Fig. 1c). We further assessed the specificity of anti-S IgG for SARS-CoV-2 S protein compared to other coronavirus
89 strains using a cell-based ELISA (see methods). Plasma IgG from subject samples but not pre-pandemic control samples bound
90 SARS-CoV-2 S protein and the common circulating D614G S protein variant¹⁸, but did not significantly bind S protein from SARS-
91 CoV-1 or MERS coronaviruses (Extended Data Fig. 1), establishing the specificity of the anti-S IgG response for SARS-CoV-2 in all
92 cohorts. However, the abundance of IgG antibodies specific for the SARS-CoV-2 nucleocapsid (N) protein, which complexes with
93 viral RNA and is involved in viral replication¹⁹ was significantly lower in both pediatric cohorts compared to the two adult cohorts

94 (Fig. 1d). The low amounts of anti-N IgG were similar in children with and without MIS-C, and the higher anti-N IgG titers in adults
95 were similar in the CPD and COVID-ARDS cohort, suggesting that generation of anti-N antibody is age- but not symptom-dependent.

96 Potential effects of age and time post-symptom onset (i.e., disease course) on the differential antibody abundance for each
97 cohort were examined. While there was no significant correlation between anti-S IgG and age among the adult subjects and the
98 pediatric MIS-C cohort, a modest but significant negative correlation between age and anti-S IgG titers was observed in the pediatric
99 non-MIS-C cohort (Fig. 1e, right). Moreover, there was a significant correlation of anti-N IgG titers with subject age within the CPD
100 group with younger adults having lower anti-N titers than older adults, while both pediatric groups had low anti-N titers across all ages
101 (Fig. 1f). Analysis of antibody abundance as a function of time post-symptom onset revealed a significant correlation between anti-S
102 IgG titers and increased time post-symptom for both pediatric groups and the adult COVID-ARDS group, suggestive of an evolving
103 response over time (Fig. 2a). No correlation with symptom onset and anti-S IgM was observed (Fig. 2b). These results show that the
104 anti-SARS-CoV-2 antibody response generated in children is predominantly anti-S IgG antibodies independent of clinical syndrome.
105 By contrast, adults generate broader antibody responses to infection in terms of isotypes and specificities, and exhibit increased
106 magnitude and breadth of the anti-S antibody response with more severe disease.

107 The functional capacity of antibodies to provide protection correlates to their neutralizing activity in blocking virus infection.
108 We developed a cell-based pseudovirus assay based on a system previously reported^{20,21} in which multi-cycle infection of red
109 fluorescent protein (RFP)-expressing vesicular stomatitis virus (VSV) pseudotyped with SARS-CoV-2 S protein is measured in the
110 presence of serially diluted plasma samples (see Methods). We validated this assay by comparing neutralizing activity of plasma
111 samples tested in the pseudovirus assay to activity measured in live virus microneutralization assay based on inhibition of cytopathic
112 effect²², and found a direct correlation in neutralizing activity calculated from the pseudovirus and live virus assay over a wide range
113 of neutralizing activity (Fig. 3a).

114 Neutralizing activity as measured by the pseudovirus assay showed differences between the four cohorts that were associated
115 with age group and/or clinical severity. The pediatric MIS-C and Non-MIS-C groups both exhibited significantly lower neutralizing
116 activity than the adult CPD and COVID-ARDS groups, while plasma from COVID-ARDS patients show the highest neutralizing
117 potency of the four groups across the dilution series (Fig. 3b,c). No differences were observed in neutralizing activity in the MIS-C

118 compared to the pediatric Non-MIS-C group (Fig. 3b,c). Only a small fraction of antibodies raised against viral antigens will have
119 neutralizing activity against the virus, which correlates with protective capacity²³. By linear regression, there was significant
120 correlation between the abundance of anti-S IgG and neutralizing activity within the CPD, MIS-C and pediatric Non-MIS-C groups,
121 albeit with a significantly lower elevation and y-intercept for MIS-C group relative to the COVID-ARDS and CPD groups (Fig. 3d).
122 Together, these results establish a significant quantitative difference in neutralizing activity of anti-SARS-CoV-2 antibodies between
123 pediatric and adult groups.

124 We examined potential effects of age and disease course on neutralizing activity in the different groups. There was no
125 correlation between neutralizing activity and patient age in either adult group (Fig. 3d). However, there was a significant decline of
126 neutralizing activity with patient age in the pediatric Non-MIS-C group (Fig. 3e, right) similar to the decrease in anti-S IgG abundance
127 with age observed during the teenage years (Fig. 1e, right). Neutralizing activity within each group did not correlate with time post-
128 symptom onset except in the severely ill COVID-ARDS group (Fig. 4a). Moreover, MIS-C patients also maintained the same titers of
129 anti-S IgG and neutralizing activity 2-4 weeks after hospital discharge based on paired analysis of the follow-up compared to the
130 retested primary sample in 10/16 (62.5%) of the patients (Fig. 4b). Together, these results indicate that lower magnitude of functional
131 antibody responses in pediatric SARS-CoV-2 infection compared to adults is age associated and not related to infection course.

132 To better define how SARS-CoV-2 antibody responses are related to age and clinical syndrome, we performed multivariable
133 linear regression analysis to control for effects of demographic and clinical covariates. Consistent with the grouped analysis (Fig. 1a-d,
134 3b), analysis of all pediatric and adult data showed that the pediatric age group is a significant predictor of lower SARS-CoV-2
135 neutralizing activity, anti-S IgM and anti-N IgG, and these relationships are independent of time post-symptom onset, clinical
136 syndrome or sex (Supplementary Table 3). In addition, ARDS was found to be a significant independent predictor of higher SARS-
137 CoV-2 neutralizing activity, anti-S IgG and anti-S IgM (Supplementary Table 3). Within the subgroup of pediatric subjects, age was
138 found to be a significant independent predictor of SARS-CoV-2 neutralizing activity (Supplementary Table 3), consistent with the
139 pairwise analysis (Fig. 3e, right). These results show that the observed relationships of age and clinical syndrome with SARS-CoV-2
140 antibody responses are independent of potentially confounding factors, including being male.

141 Together, our results show quantitative and qualitative differences in the anti-SARS-CoV-2-specific antibody response across
142 the spectrum of infection in children compared to adults. Children exhibited a SARS-CoV-2-specific antibody response that was
143 largely limited to IgG anti-S antibodies with the lowest overall level of neutralizing activity compared to adult COVID-19 cohorts. In
144 addition, children with different disease severities (*i.e.* with or without MIS-C) exhibited similar antibody profiles, while in the adult
145 cohorts, those with the most severe disease (ARDS) had higher abundance, breadth and neutralizing activity of anti-SARS-CoV-2
146 antibodies compared to adults who recovered from mild disease. While there was an association with increased amounts of anti-S IgG
147 and time post-symptom onset, age remained the major factor distinguishing antibody profiles. Additionally, the durable responses seen
148 in follow-up samples from MIS-C subjects provide evidence for relative stability of antibody abundance over a period of weeks. These
149 findings suggest distinct primary SARS-CoV-2 infection courses and immune responses in children and adults.

150 Optimal protection to viral respiratory tract infections is mediated by virus-specific immunological memory developed during
151 previous exposures²⁴. The majority of primary exposures, especially to viral respiratory pathogens which are ubiquitous in the
152 population, occur during infancy and childhood and virus-specific memory is established by adult life^{25,26}. Consequently, it is largely
153 unknown how primary immune responses to viral pathogens may differ between children and adults. The sudden and widespread
154 emergence of SARS-CoV-2 as a novel pathogen enables the study of primary immune responses across all ages. The reduced
155 respiratory symptoms and low incidence of ARDS in the pediatric population² suggest a distinct infection course, possibly due to
156 lower expression of the viral receptor (ACE2) in pediatric airway epithelial cells²⁷ or a more robust innate immune response in
157 children²⁸⁻³⁰. A milder infection course in pediatric groups is further consistent with lower abundance of anti-N-specific antibodies
158 identified here, as release of N proteins requires lysis of virally infected cells. The age association of anti-N antibodies in the adult
159 CPD group is consistent with the age-associated risk for more severe and prolonged disease from SARS-CoV-2 infection. While
160 current platforms to determine prior infection with SARS-CoV-2 rely heavily on the detection of anti-N IgG, our results suggest that
161 these testing platforms may have decreased sensitivity for assessing previous infections among the pediatric population.

162 The reduced functional antibody response in children compared to adults could also be due to efficacious immune-mediated
163 viral clearance resulting in fewer respiratory symptoms and severe illness. The presence of SARS-CoV-2-specific T cells in the
164 peripheral blood of recovered and COVID-ARDS adults has been demonstrated in multiple cohorts³¹⁻³³, though the protective capacity

165 of these T cells is unclear. The pediatric T cell response to SARS-CoV-2 requires investigation but may exceed the adult responses
166 due to an increased number of naïve T cells available to respond to new pathogens³⁴, or more recently acquired T cell memory to
167 related coronavirus strains³⁵ due to children experiencing more respiratory illnesses. The IgG predominance in the majority of children
168 examined here is consistent with pre-existing immunological memory. Interestingly, less severe manifestations of COVID-19 have
169 been associated with a more coordinated adaptive immune responses in adults³⁶, suggesting that the quality and quantity of the
170 immune response is important for protection from severe disease, which are important future areas of investigation for understanding
171 the immune response to SARS-CoV-2 infection in children.

172 The similar antibody profiles in children with and without MIS-C suggests that the adaptive immune response per se, is not
173 associated with MIS-C pathogenesis. However, reduced neutralizing activity may predispose children to develop low-level, persistent
174 infection in other sites resulting in MIS-C. Children can present with gastrointestinal symptoms rather than respiratory illness and
175 demonstrate prolonged fecal shedding of the virus³⁷. Alternately, the presence of non-neutralizing anti-S Abs could lead to antibody-
176 dependent enhancement of infection (ADE) known to occur in viral infections including SARS-CoV-1³⁸. Additionally, autoreactive
177 antibodies recently identified in children with MIS-C may promote aberrant immune responses leading to systemic inflammation^{29,30}.
178 Further studies delineating the differences in adult and pediatric immune responses to SARS-CoV-2 are warranted to define how
179 protection or pathology is mediated in response to this pathogen. In summary, our results suggest a distinct infection course and
180 immune response in children independent of whether they develop MIS-C, with implications for developing age-targeted strategies for
181 testing and protecting the population.

182 **ACKNOWLEDGEMENTS**

183 We thank F. Cosset for the donation of Vero E6 cells. We wish to express our gratitude to the Medical ICU nurse champions, C.
184 Garcellano, T. Drukdak, H. Avila Raymundo, L. Wagner, and R. Lee, who led the efforts to obtain patient samples for the adult
185 ARDS patients, to E. Hernandez and L. Gomez for their roles as clinical coordinators, and to the nurses and clinical staff in the
186 Pediatric Intensive Care Unit of MSCHONY. We acknowledge the dedication, commitment, and sacrifice of the other nurses,
187 providers, and personnel who helped care for these patients during the COVID-19 crisis. We acknowledge the suffering and
188 loss of our COVID-19 patients and of their families and our community.

189 **Funding/Support**

190 This work was supported by NIH grants AI128949, AI100119, AI106697 awarded to D.L.F., NIH grants AI121349, NS091263,
191 NS105699, and AI146980 awarded to M.P., and AI114736 awarded to A.M. S.W. is supported by NIH K08DK122130; T.J.C. is
192 supported by NIH K23 AI141686.

193 **Role of the Funder:** The funders/sponsors had no role in the design and conduct of the study; collection, management,
194 analysis, and interpretation of the data; preparation, review, or approval of the manuscript; and decision to submit the
195 manuscript for publication.

196 **AUTHOR CONTRIBUTIONS**

197 All authors meet authorship criteria and approve of publication. S.P.W., T.J.C., M.P. and D.L.F., A.M., and E.H. conceived and
198 designed the study and assays, wrote and/or edited the paper. T.J.C., M.R.B., D.L.F., E.M., J.M., E.I., coordinated sample acquisition,
199 recruited and consented MIS-C and COVID-ARDS patients. T.J.C., J.D-P., S.P.W., E.M., J.M. and M.R.B. performed compilation
200 and analysis of clinical data from MIS-C and COVID-ARDS patients. E.H., and Z.C.B. recruited and consented convalescent plasma
201 donors. S.P.W. and Z.C.B. performed compilation and analysis of data from the convalescent plasma study. F.L.C., S.A.F, M.C., and
202 S.P.W. performed collection, isolation and storage of samples from convalescent plasma donors. P.A.S, S.B.W., P.D., J.G., E.I., R.M.,
203 and M.M.L.P. performed collection, isolation and storage of samples from COVID-ARDS patients. E.H., S.W. K.E.H, F.D.Z. and
204 W.L. established and performed ELISA assays for quantification of anti-SARS-CoV-2 S and N protein IgG, IgM, and IgA from
205 human serum and plasma. M.P., A.M., F.T.B, D.S. and Y.Z. established and performed SARS-CoV-2 S protein pseudovirus
206 neutralization assays. C.M., B.H., and D.D. established and performed the SARS-CoV-2 live virus neutralization assay. S.P.W., D.L.F
207 and T.J.C. performed compilation and analysis of data from the ELISA, pseudovirus neutralization and live virus neutralization
208 assays.

209

210 **Competing Interests statement**

211 The authors have no conflicts with regard to this work.

212 REFERENCES

213 1. Dong, Y., *et al.* Epidemiology of COVID-19 Among Children in China. *Pediatrics* **145**(2020).
214 2. Wu, Z. & McGoogan, J.M. Characteristics of and Important Lessons From the Coronavirus Disease 2019 (COVID-19)
215 Outbreak in China: Summary of a Report of 72314 Cases From the Chinese Center for Disease Control and Prevention.
216 *JAMA* **323**, 1239-1242 (2020).
217 3. Cheung, E.W., *et al.* Multisystem Inflammatory Syndrome Related to COVID-19 in Previously Healthy Children and
218 Adolescents in New York City. *JAMA* **324**, 294-296 (2020).
219 4. Feldstein, L.R., *et al.* Multisystem Inflammatory Syndrome in U.S. Children and Adolescents. *N Engl J Med* **383**, 334-346
220 (2020).
221 5. Whittaker, E., *et al.* Clinical Characteristics of 58 Children With a Pediatric Inflammatory Multisystem Syndrome Temporally
222 Associated With SARS-CoV-2. *JAMA* **324**, 259-269 (2020).
223 6. Singh, A.K., *et al.* Prevalence of co-morbidities and their association with mortality in patients with COVID-19: A systematic
224 review and meta-analysis. *Diabetes Obes Metab* (2020).doi: 10.1111/dom.14124
225 7. Lanzavecchia, A., Fruhwirth, A., Perez, L. & Corti, D. Antibody-guided vaccine design: identification of protective epitopes.
226 *Curr Opin Immunol* **41**, 62-67 (2016).
227 8. Corti, D. & Lanzavecchia, A. Broadly neutralizing antiviral antibodies. *Annu Rev Immunol* **31**, 705-742 (2013).
228 9. Wang, X., *et al.* Neutralizing Antibodies Responses to SARS-CoV-2 in COVID-19 Inpatients and Convalescent Patients. *Clin*
229 *Infect Dis* (2020).doi: 10.1093/cid/ciaa721
230 10. Ni, L., *et al.* Detection of SARS-CoV-2-Specific Humoral and Cellular Immunity in COVID-19 Convalescent Individuals.
231 *Immunity* **52**, 971-977 e973 (2020).
232 11. Long, Q.X., *et al.* Antibody responses to SARS-CoV-2 in patients with COVID-19. *Nat Med* **26**, 845-848 (2020).
233 12. Amanat, F., *et al.* A serological assay to detect SARS-CoV-2 seroconversion in humans. *Nat Med* **26**, 1033-1036 (2020).
234 13. Bloch, E.M., *et al.* Deployment of convalescent plasma for the prevention and treatment of COVID-19. *J Clin Invest* **130**,
235 2757-2765 (2020).
236 14. Amanat, F. & Krammer, F. SARS-CoV-2 Vaccines: Status Report. *Immunity* **52**, 583-589 (2020).
237 15. Huang, A.T., *et al.* A systematic review of antibody mediated immunity to coronaviruses: kinetics, correlates of protection, and
238 association with severity. *Nat Commun* **11**, 4704 (2020).
239 16. Cummings, M.J., *et al.* Epidemiology, clinical course, and outcomes of critically ill adults with COVID-19 in New York City: a
240 prospective cohort study. *Lancet* **395**, 1763-1770 (2020).
241 17. Zachariah, P., *et al.* Epidemiology, Clinical Features, and Disease Severity in Patients With Coronavirus Disease 2019
242 (COVID-19) in a Children's Hospital in New York City, New York. *JAMA Pediatr*, e202430 (2020).
243 18. Korber, B., *et al.* Tracking Changes in SARS-CoV-2 Spike: Evidence that D614G Increases Infectivity of the COVID-19 Virus.
244 *Cell* **182**, 812-827 e819 (2020).
245 19. Cong, Y., *et al.* Nucleocapsid Protein Recruitment to Replication-Transcription Complexes Plays a Crucial Role in Coronaviral
246 Life Cycle. *J Virol* **94**, e01925-19 (2020).doi: 10.1128/JVI.01925-19
247 20. Talekar, A., *et al.* Rapid screening for entry inhibitors of highly pathogenic viruses under low-level biocontainment. *PLoS One*
248 **7**, e30538 (2012).

- 249 21. Porotto, M., *et al.* Simulating henipavirus multicycle replication in a screening assay leads to identification of a promising
250 candidate for therapy. *J Virol* **83**, 5148-5155 (2009).
- 251 22. Chan, K.H., *et al.* Cross-reactive antibodies in convalescent SARS patients' sera against the emerging novel human
252 coronavirus EMC (2012) by both immunofluorescent and neutralizing antibody tests. *J Infect* **67**, 130-140 (2013).
- 253 23. Gao, Q., *et al.* Development of an inactivated vaccine candidate for SARS-CoV-2. *Science* **369**, 77-81 (2020).
- 254 24. Kohlmeier, J.E. & Woodland, D.L. Immunity to respiratory viruses. *Annu Rev Immunol* **27**, 61-82 (2009).
- 255 25. He, X.S., *et al.* Analysis of the frequencies and of the memory T cell phenotypes of human CD8+ T cells specific for influenza
256 A viruses. *J Infect Dis* **187**, 1075-1084 (2003).
- 257 26. PrabhuDas, M., *et al.* Challenges in infant immunity: implications for responses to infection and vaccines. *Nat Immunol* **12**,
258 189-194 (2011).
- 259 27. Bunyavanich, S., Do, A. & Vicencio, A. Nasal Gene Expression of Angiotensin-Converting Enzyme 2 in Children and Adults.
260 *JAMA* **323**, 2427-2429 (2020).
- 261 28. Pierce, C.A., *et al.* Immune responses to SARS-CoV-2 infection in hospitalized pediatric and adult patients. *Sci Transl Med*
262 **12**, eabd5487 (2020).
- 263 29. Gruber, C.N., *et al.* Mapping Systemic Inflammation and Antibody Responses in Multisystem Inflammatory Syndrome in
264 Children (MIS-C). *Cell* (2020).doi: 10.1016/j.cell.2020.09.034
- 265 30. Consiglio, C.R., *et al.* The Immunology of Multisystem Inflammatory Syndrome in Children with COVID-19. *Cell* (2020).doi:
266 10.1016/j.cell.2020.09.016
- 267 31. Weiskopf, D., *et al.* Phenotype and kinetics of SARS-CoV-2-specific T cells in COVID-19 patients with acute respiratory
268 distress syndrome. *Sci Immunol* **5**, eabd2071 (2020).
- 269 32. Grifoni, A., *et al.* Targets of T Cell Responses to SARS-CoV-2 Coronavirus in Humans with COVID-19 Disease and
270 Unexposed Individuals. *Cell* **181**, 1489-1501 e1415 (2020).
- 271 33. Sekine, T., *et al.* Robust T Cell Immunity in Convalescent Individuals with Asymptomatic or Mild COVID-19. *Cell* **183**, 158-168
272 e114 (2020).
- 273 34. Kumar, B.V., Connors, T.J. & Farber, D.L. Human T Cell Development, Localization, and Function throughout Life. *Immunity*
274 **48**, 202-213 (2018).
- 275 35. Mateus, J., *et al.* Selective and cross-reactive SARS-CoV-2 T cell epitopes in unexposed humans. *Science* **370**, 89-94
276 (2020).
- 277 36. Moderbacher, C., *et al.* Antigen-Specific Adaptive Immunity to SARS-CoV-2 in Acute COVID-19 and Associations with Age
278 and Disease Severity. *Cell* (2020).doi:10.1016/j.cell.2020.09.038
- 279 37. Xu, Y., *et al.* Characteristics of pediatric SARS-CoV-2 infection and potential evidence for persistent fecal viral shedding. *Nat*
280 *Med* **26**, 502-505 (2020).
- 281 38. Iwasaki, A. & Yang, Y. The potential danger of suboptimal antibody responses in COVID-19. *Nat Rev Immunol* **20**, 339-341
282 (2020).
- 283
- 284

285 **FIGURE LEGENDS**

286 **Figure 1. Children with and without MIS-C exhibit distinct SARS-CoV-2 antibody profiles compared to adults with COVID-**

287 **19.** Levels of antibodies to SARS-CoV-2 spike (S) and nucleocapsid (N) proteins were measured using serial dilutions of patient
288 plasma in an indirect ELISA assay to detect anti-S IgG (a), anti-S IgM (b), anti-S Ig A (c) and anti-N IgG (d). Shown is the
289 absorbance sum across 6 serial 1:4 plasma dilutions from adult convalescent plasma donors (CPD, open black squares, n=19); adult
290 patients with COVID-19 induced acute respiratory distress syndrome (COVID-ARDS, closed red squares, n=13); pediatric patients
291 with a history of SARS-CoV-2 infection but not MIS-C (Non-MIS-C, open blue circles, n=31); patients with MIS-C (MIS-C, closed
292 green circles, n=16); and control plasma from pre-pandemic donors (Neg, grey triangles, n=10). Black bar indicates the
293 median+interquartile range. P values were calculated by one-way ANOVA with Sidak's multiple comparisons test. Anti-S IgG (a),
294 CPD vs. COVID ARDS: $P=1.32 \times 10^{-4}$, CPD vs. Ped non-MIS-C: $P=0.59$, COVID ARDS vs. MIS-C: $P=8.53 \times 10^{-6}$, Ped non-MIS-C vs.
295 MIS-C: $P=0.24$. Anti-S IgM (b), CPD vs. COVID ARDS: $P=6.93 \times 10^{-5}$, CPD vs. Ped non-MIS-C: $P=0.33$, COVID ARDS vs. MIS-C:
296 $P=2.54 \times 10^{-6}$, Ped non-MIS-C vs. MIS-C: $P=0.99$. Anti-S IgA (c), CPD vs. COVID ARDS: $P=3.82 \times 10^{-7}$, CPD vs. Ped non-MIS-C:
297 $P=0.08$, COVID ARDS vs. MIS-C: $P=9.06 \times 10^{-7}$, Ped non-MIS-C vs. MIS-C: $P=0.11$. Anti-N IgG (d), CPD vs. COVID ARDS:
298 $P=0.93$, CPD vs. Ped non-MIS-C: $P=3.31 \times 10^{-5}$, COVID ARDS vs. MIS-C: $P=3.88 \times 10^{-5}$, Ped non-MIS-C vs. MIS-C: $P=0.99$.
299 Significance is indicated as * $P < 0.05$, ** $P < 0.01$, *** $P < 0.001$ or $P > 0.05$ (ns). For anti-S IgG (e) and anti-N IgG (f), subject antibody
300 levels are also plotted against patient age within the adult (left) and pediatric cohorts (right) with the best fit lines and P values
301 calculated using simple linear regression. Anti-S IgG vs. Age (Ped non-MIS-C: $R^2=0.23$, slope=-0.077, y-int=2.70). Anti-N IgG vs.
302 Age (CPD: $R^2=0.34$, slope=0.023, y-int=0.12).

303 **Figure 2. Relationship of anti-S IgG and IgM levels with time post symptom onset for pediatric and adult cohorts.** Levels of
304 anti-S IgG (a), and IgM (b) were plotted against the time post symptom onset for those subjects that were symptomatic either with
305 COVID-19 or MIS-C. The adult groups, CPD (open black squares, n=19) and COVID-ARDS closed red squares, n=13) are plotted on
306 the left and the pediatric groups, MIS-C (closed green circles, n=16) and non-MIS-C (open blue circles, n=16) are plotted on the right
307 with the best fit line and P value, reported to 4 decimal places, was calculated using simple linear regression. Anti-S IgG vs. Time post

308 symptom onset (COVID-ARDS: $R^2=0.39$, slope=0.11, y-int=1.59; MIS-C: $R^2=0.25$, slope=0.055, y-int=1.87; Ped non-MIS-C:
309 $R^2=0.30$, slope=0.021, y-int=1.29).

310 **Figure 3. Reduced SARS-CoV-2 neutralizing activity in children with and without MIS-C compared to adults with mild and**
311 **severe COVID-19.** a, Plasma neutralizing activity in the pseudovirus assay was correlated with the end point titers in a live virus
312 microneutralization assay based on inhibition of cytopathic effect (n=13, see methods). b, Neutralizing activity for SARS-CoV-2-
313 specific antibodies was determined using the pseudovirus assay (see methods). Neutralizing activity is shown from adult convalescent
314 plasma donors (CPD, open black squares, n=19); adult patients with COVID-19 induced acute respiratory distress syndrome (COVID-
315 ARDS, closed red squares, n=13); pediatric patients with a history of SARS-CoV-2 infection but not MIS-C (Non-MIS-C, open blue
316 circles, n=31); patients with MIS-C (MIS-C, closed green circles, n=16); and control plasma from pre-pandemic donors (Neg, grey
317 triangles, n=10). Black bar indicates the median+interquartile range. The P values were calculated by one-way ANOVA with Sidak's
318 multiple comparisons test (CPD vs. COVID ARDS: $P=0.019$, CPD vs. Ped non-MIS-C: $P=0.0031$, COVID ARDS vs. MIS-C:
319 $P=3.35 \times 10^{-6}$, Ped non-MIS-C vs. MIS-C: $P=1.0$). Significance is indicated as * $P < 0.05$, ** $P < 0.01$, *** $P < 0.001$ or $P > 0.05$ (ns).
320 Shown (c) are the percent inhibition values of S-protein mediated pseudoviral replication plotted against the plasma dilution factors
321 for all subjects in each group. Neutralizing activity is plotted against anti-S IgG levels (d) and patient age (e) within the adult (left) and
322 pediatric cohorts (right). The best fit lines and P values (reported to 4 decimal places), were calculated using simple linear regression.
323 Neutralizing activity vs. anti-S IgG (CPD: $R^2=0.29$, slope=0.36, y-int=0.88; MIS-C: $R^2=0.51$, slope=0.38, y-int=0.43; Ped non-MIS-
324 C: $R^2=0.21$, slope=0.22, y-int=0.86). Neutralizing activity vs. age (Ped non-MIS-C: $R^2=0.20$, slope=-0.034, y-int=1.64).

325 **Figure 4. Relationship of anti-SARS-CoV-2 neutralizing activity with time post symptom onset.** a, Levels of neutralization
326 activity were plotted against the time post symptom onset for those subjects that were symptomatic either with COVID-19 or MIS-C.
327 The adult groups, CPD (open black squares, n=19) and COVID-ARDS closed red squares, n=13) are plotted on the left and the
328 pediatric groups, MIS-C (closed green circles, n=16) and non-MIS-C (open blue circles, n=16) are plotted on the right with the best fit
329 line and P value calculated using simple linear regression (COVID-ARDS: $R^2=0.36$, slope=0.040, y-int=1.34). b, The anti-S IgG
330 levels (left) and neutralizing activity (right) of MIS-C subjects (n=10) during the acute phase of illness and at a follow-up visit 2-4
331 weeks after hospital discharge. The P values were calculated by two way paired t-test.

Table 1. Demographic and Clinical Data

	Adults		Pediatric		P Value
	CPD (n=19)	COVID-ARDS (n=13)	MIS-C (n=16)	Non MIS-C (n=31)	
Demographics					
Age, years, median (range)	45 (28-69)	62 (19-84)	11 (4-17)	11 (3-18)	
Sex, male (%)	10 (53%)	11 (85%)	7 (44%)	17 (55%)	
Body Mass Index, median (IQR)	na	33.8 (28.4-36.1)	19.1 (17.3-25.5)	19.3 (16.9-22.3)	
Race or Ethnic Group (%)^a					
Hispanic or Latino	1 (5%)	4 (31%)	4 (25%)	13 (42%)	
Black or African American	0	3 (23%)	7 (44%)	4 (13%)	
White	10 (53%)	2 (15%)	7 (44%)	15 (48%)	
Asian	6 (32%)	0	0	0	
Pacific Islander	2 (11%)	0	0	0	
Other or Unknown	1 (5%)	5 (38%)	1 (6%)	7 (23%)	
Clinical Characteristics					
SARS-CoV-2 PCR Positive (%) ^b	na	13 (100%)	8 (50%)	22 (71%)	
Asymptomatic (%)	na	0	0	15 (48%)	
Days Post Symptom Onset, median (IQR) ^c	24 (19-37)	16 (14-21)	6 (4-7)	29 (17-44) ^d	
SOFA Score ^e , median (IQR) ^f	na	11 (9.5-14)	4 (3-7)	na	
Acute Respiratory Distress Syndrome (%)	na	13 (100%)	1 (6%)	1 (3%)	
In-hospital Mortality (%) ^g	na	6 (46%)	0 (0%)	0 (0%)	
Laboratory Results, median (IQR)^{f,h,i}					
Absolute Neutrophil Count, x10(3)/μL	na	14.7 (9.1-25.2)	8.9 (7.2-16.4)	5.0 (3.2-8.0)	0.0005
Absolute Lymphocyte Count x10(3)/μL	na	0.9 (0.7-1.4)	0.8 (0.4-1.5)	2.0 (1.3-2.8)	0.0001
Albumin, g/dL	na	3.4 (2.8-3.5)	3.4 (2.6-4.2)	4.6 (4.3-4.9)	2.6x10 ⁻⁷
D-dimer, μg/mL	na	7.9 (1.7-16.1)	3.1 (1.7-4.3)	na	0.07
Ferritin, ng/mL	na	1933 (971-2693)	521 (298-998)	na	0.002
High Sensitivity CRP, mg/L	na	128 (69-207)	214 (47-300)	na	0.56
Interleukin-6, pg/mL	na	82 (56-315)	219 (54-315)	na	0.63
Lactate Dehydrogenase, U/L	na	777 (638-1379)	268 (229-373)	na	0.0003
Procalcitonin, ng/mL	na	0.4 (0.3-2.0)	8.8 (2.1-61.6)	na	0.002
Troponin T, high sensitivity, ng/L	na	24 (16-59)	20 (6-92)	na	0.85
Abbreviations: CPD, convalescent plasma donor; ARDS, Acute Respiratory Distress Syndrome; MIS-C Multisystem Inflammatory Syndrome in Children; SOFA, Sequential Organ Failure Assessment; IQR, Interquartile Range; PCR, Polymerase chain reaction; CRP, C-Reactive Protein					
a Individuals included in all groups for which they identified					
b Indeterminate tests were treated as positive					
c Respiratory symptoms/COVID-19 symptoms for CPD/ARDS groups and symptoms of MIS-C for MIS-C group					
d Subjective reporting of days post symptom onset for those presenting with symptoms or total days after confirmed COVID-19 exposure (reportable data available for n=16 subjects)					
e Pediatric and Adult specific scoring applied to groups; not meant for direct comparison					
f Day of admission for MIS-C, day of intubation for COVID-ARDS, day of PCR or Serology sample testing for Non MIS-C					
g 30 Day In-hospital mortality, 4 patients remain hospitalized					
h Values above upper limit entered as; D-Dimer (20 mg/mL), Ferritin (100,000 ng/mL), CRP (200 mg/L), Interleukin-6 (315 pg/mL), Lactate Dehydrogenase (5000 U/L)					
i Statistical testing for Absolute Neutrophil Count, Absolute Lymphocyte Count and Albumin done via Kruskal-Wallis one-way analysis of variance. Statistical testing for all other laboratory results done by two-tailed Mann-Whitney test. P values were calculated to 4 decimal places. Absolute Neutrophil Count and Absolute Lymphocyte Count; n=13 COVID-ARDS, n=16 MIS-C, n=27 Non MIS-C. Albumin; n=13 COVID-ARDS, n=16 MIS-C, n=15 Non MIS-C. D-dimer and Ferritin; n=13 COVID-ARDS, n=16 MIS-C. For High Sensitivity CRP; n=12 COVID-ARDS, n=16 MIS-C. Interleukin-6 and Troponin; n=11 COVID-ARDS, n=16 MIS-C. Lactate Dehydrogenase; n=12 COVID-ARDS, n=15 MIS-C. Procalcitonin; n= 13 COVID-ARDS, n=12 MIS-C.					

332 **METHODS**

333 **Subjects**

334 We recruited a total of 79 subjects from MSCHONY and CUIMC/NYP who represented distinct clinical
335 manifestations of SARS-CoV-2 infection and different age groups divided into four cohorts: 1.
336 Individuals (n=19) donating blood as part of our institution's convalescent plasma trial (convalescent
337 plasma donors, CPD) following a history of recent illness consistent with COVID-19 but not requiring
338 hospitalization and subsequently identified as positive for anti-SARS-CoV-2 antibodies; 2. Patients with
339 severe COVID-19 and ARDS (n=13) who tested positive for SARS-CoV-2 by polymerase chain
340 reaction (PCR) from nasopharyngeal swabs; 3. Pediatric patients with MIS-C (n=16) and confirmed
341 SARS-CoV-2 antibody positive serology; and 4. Pediatric patients without MIS-C (n=31) receiving
342 medical attention at CUIMC/NYP and confirmed to have active or previous SARS-CoV-2 infection by
343 PCR from nasopharyngeal swabs or antibody positive serology. ARDS was defined by clinical
344 consensus criteria; including infiltrates on chest radiograph and a PaO₂/FiO₂ ratio of less than 300, or
345 pediatric criteria equivalent^{39,40}. MIS-C was defined using the Center for Disease Control definition;
346 <21 years of age, fever >38°C for >24 h, laboratory evidence of inflammation, hospital admission,
347 multisystem involvement, no alternative plausible diagnosis, and positive SARS-Cov-2 serology⁴¹.
348 Sequential Organ Failure Assessment (SOFA) scores were calculated on all hospitalized subjects using
349 previously validated adult and pediatric score tools to provide additional clinical insight into subject
350 disease severity⁴²⁻⁴⁴. This study was approved by the Institutional Review Board at CUIMC. Written
351 consent was obtained from CPD subjects. Due to the limitations placed on direct contact with infected
352 subjects and a need to conserve personal protective equipment, verbal informed consent was obtained
353 from surrogates of critically ill COVID-ARDS subjects and verbal parental consent was obtained for
354 MIS-C subjects. Biospecimens and data from Non-MIS-C pediatric patients were obtained from the
355 Columbia University Biobank (CUB).

356 **Sample Processing**

357 Blood samples were obtained at time of outpatient donation for CPD subjects, at time of admission for
358 MIS-C subjects, during clinical care for pediatric Non-MIS-C subjects and following diagnosis of
359 ARDS for COVID-ARDS patients. Plasma was isolated from whole blood via centrifugation. Aliquots
360 were frozen at -80°C prior to analysis.

361 **Purification of SARS-CoV-2 viral proteins**

362 The ectodomain of the SARS-CoV-2 spike trimer⁴⁵ was cloned into mammalian expression vector
363 pCAGGS (Addgene), with a fold-on tag followed by 6xHis tag and Strep tag II at the C-terminal. This
364 expression vector was transiently transfected into HEK293F cells and the spike trimer secreted in the
365 supernatant was purified 3-5 days post transfection by metal-affinity chromatography using an Ni-NTA
366 (Qiagen) column. SARS-CoV-2 nucleocapsid protein (N) was cloned into pET28a(+) vector (Millipore-
367 Sigma) with an AAALe linker and 6xHis tag at the C-terminal. The NP construct was then used to
368 transform into *Escherichia coli* BL21 (DE3) pLysS cells and the target protein was produced and
369 purified from the bacterial lysate by metal affinity chromatography using an Ni-NTA (Qiagen) column,
370 followed by size-exclusion chromatography on a Superdex 200 10/300 GL column.

371 **Enzyme-linked immunosorbent assay (ELISA) for detection of virus-specific antibodies**

372 SARS-CoV-2 spike trimer and N were coated on 96-well ELISA plates at 4 °C overnight, and unbound
373 proteins were then removed washing with PBS, following by blocking with PBS/3% non-fat dry milk.
374 Plasma samples were serially diluted in PBST (0.1% Tween-20 in PBS) + 10% bovine calf serum
375 starting with 1:100, and five successive four-fold dilutions into each well of the coated plate which was
376 incubated at 37 °C for 1 h, followed by washing 6 times with PBST. Peroxidase affiniPure goat anti-
377 human IgG (H+L) antibody (1:3,000 dilution), anti-human IgM antibody (1:10,000 dilution) (Jackson
378 Immune Research), or anti-human IgA antibody (1:5,000 dilution) (ThermoFisher) was subsequently
379 added into each well and incubated for 1 h at 37 °C, washed and Tetramethylbenzidine substrate (Sigma)
380 was added and the reaction was stopped using 1 M sulfuric acid. Absorbance was measured at 450 nm
381 and expressed as an optical density, or OD₄₅₀ value. Identical serial dilutions were performed for all
382 samples with no missing titrations.

383 **Pseudovirus neutralization assay**

384 We adapted a pseudovirus-based neutralization strategy we previously developed to measure inhibition
385 of infection by high biocontainment enveloped viruses in a large number of samples under low-level
386 biocontainment^{20,21}. For this assay, SARS-CoV-2 S protein is pseudotyped onto recombinant vesicular
387 stomatitis virus (VSV) that expresses red fluorescent protein (RFP) but does not express the VSV
388 attachment protein, G (VSV-ΔG-RFP). Initially, VSV-ΔG-RFP pseudotyped with VSV G is used to
389 infect 293T (human kidney epithelial) cells that were co-transfected with full-length codon optimized
390 SARS-CoV-2 S-protein (Epoch Life Science), the viral entry receptor ACE2 (Epoch Life Science) and
391 green-fluorescent protein (GFP). Infected HEK293T cells are then mixed at a 2 to 1 ratio with Vero
392 (African green monkey kidney) cells, which have high endogenous expression of ACE2⁴⁶. The cells are

393 then combined with diluted serum or plasma in 96-well plates. During the assay, infected S protein-
394 expressing HEK293T cells generate VSV-ΔG-RFP viruses that bear S protein which subsequently
395 infects and drives RFP expression in Vero cells and undergo multiple cycles of entry and budding in the
396 HEK293T cells due to the co-expression of S protein with ACE2. The GFP and RFP signals are
397 measured 24–48 h after plating (Infinite M1000 PRO microplate reader, Tecan), resulting in robust
398 amplification of the S protein pseudovirus-driven RFP signal between 24–48 h. Inhibition of RFP signal
399 amplification indicates S protein neutralizing activity in patient plasma (Extended Data Fig. 1).
400 Identical, five-fold serial dilutions were performed for all samples and there were no missing titration
401 data points for any of the samples.

402 **SARS-CoV-2 viral stock production**

403 SARS-CoV-2 (2019-nCoV/USA_WA1/2020) was kindly provided to B.H. by World Reference Center
404 for Emerging Viruses and Arboviruses (WRCEVA). To generate virus stocks, Vero E6 cells (kindly
405 provided by F. Cosset, CIRI - International Center for Infectiology Research, Inserm) were inoculated
406 with virus at a MOI of 0.01. The virus-containing medium was harvested at 72 h post infection, clarified
407 by low-speed centrifugation, aliquoted, and stored at -80°C. Virus stock was quantified by limiting
408 dilution plaque assay on Vero E6 cells as described^{47,48}.

409 **Live virus neutralization assay**

410 Two-fold dilutions of plasma in 50 μL of Dulbecco's Modified Eagle Media (DMEM) were incubated
411 with 200 plaque forming units (PFU) of SARS-CoV-2 in 50 μL of DMEM for 30 min at 4 °C. 100 μL of
412 DMEM 4%FBS containing 4×10^4 Vero E6 cells were added on the top of the former mix in order to
413 have final dilution of sera from 1:50 to 1:6400 (4 wells per dilution). Cells were then incubated for 3
414 days at 37 °C, 5% CO₂. Cytopathic effect was revealed by crystal violet staining, and scored by an
415 observer blinded to the study design and sample identity. Neutralization end point titers were expressed
416 as the value of the last serum dilution that completely inhibited virus-induced cytopathic effect.

417 **Quantitation of antibody titrations in ELISA and neutralization assays**

418 For quantitation of neutralization titers in the pseudovirus assay, RFP signal driven by the pseudovirus
419 normalized to the GFP signal derived from the SARS-Cov-2 S protein and ACE2 transfected cells was
420 measured at 24 and 48 h; the ratio of normalized RFP at 48 h (RFP48) to normalized RFP at 24 h
421 (RFP24) was calculated. This ratio provides a read-out of multicycle infection of the S protein/ACE2
422 transfected cell monolayer by S protein-bearing pseudoviruses. Neutralizing activity for each sample
423 was calculated by taking the sum of the reciprocal of the RFP48/RFP24 ratio at all 6 plasma dilutions for

424 each sample as described⁴⁹, and also by percent inhibition of multicycle replication at each dilution
425 calculated based on the RFP48/RFP24 ratio of the sample, control wells of maximal multicycle
426 replication without inhibition (MAX) and control wells with 100% inhibition of multicycle replication
427 using a lipidated SARS-CoV-2 derived peptide (MIN)^{50,51}. The equation for % inhibition of multicycle
428 replication: $100 \times (1 - (\text{sample} - \text{MAX}) / (\text{MAX} - \text{MIN}))$.

429 **Statistical analysis**

430 All statistical analysis was performed using Prism software version 8.4.3 (GraphPad). Comparisons of
431 clinical data between groups was performed using the Mann–Whitney U test and one-way Analysis of
432 Variance (ANOVA) and Dunn’s multiple comparisons test. Comparisons of antibody levels and
433 neutralization activity were performed using one-way ANOVA and Tukey’s multiple comparisons test.
434 Pairwise correlation analysis was performed using simple linear regression. Multiple linear regression
435 analysis was performed on the combined adult and pediatric data as well as the adult and pediatric
436 cohorts individually. For all analyses, outcome variables included the abundance of anti-S IgG, anti-S
437 IgM, anti-N IgG and SARS-CoV-2 neutralizing activity. For the combined adult and pediatric dataset,
438 the independent variable is pediatric age group (‘Pediatric’) and covariates include sex, clinical
439 syndrome and time post symptom onset (days). For the adult and pediatric subgroup analyses, the
440 independent variables are clinical syndrome and age (years), and covariates include sex and time post
441 symptom onset (days). For each variable, P values were calculated using the *t* statistic with two-sided
442 hypothesis testing.

443

444 **Data availability statement**

445 The raw data analyzed for this study are provided as Source Data. Additional supporting data are
446 available from the authors upon request.

447 **Code availability statement**

448 N/A

449

450 **Methods-only References**

- 451 39. Ranieri, V.M., *et al.* Acute respiratory distress syndrome: the Berlin Definition. *JAMA* **307**, 2526-
452 2533 (2012).
- 453 40. Khemani, R.G., Smith, L.S., Zimmerman, J.J., Erickson, S. & Pediatric Acute Lung Injury
454 Consensus Conference, G. Pediatric acute respiratory distress syndrome: definition, incidence,
455 and epidemiology: proceedings from the Pediatric Acute Lung Injury Consensus Conference.
456 *Pediatr Crit Care Med* **16**, S23-40 (2015).
- 457 41. CDC. Multisystem Inflammatory Syndrome in Children (MIS-C) Associated with Coronavirus
458 Disease 2019 (COVID-19). Vol. 2020 Health Alert Network (Health and Human Services, 2020).
- 459 42. Singer, M., *et al.* The Third International Consensus Definitions for Sepsis and Septic Shock
460 (Sepsis-3). *JAMA* **315**, 801-810 (2016).
- 461 43. Matics, T.J. & Sanchez-Pinto, L.N. Adaptation and Validation of a Pediatric Sequential Organ
462 Failure Assessment Score and Evaluation of the Sepsis-3 Definitions in Critically Ill Children.
463 *JAMA Pediatr* **171**, e172352 (2017).
- 464 44. Vasilevskis, E.E., *et al.* Validity of a Modified Sequential Organ Failure Assessment Score Using
465 the Richmond Agitation-Sedation Scale. *Crit Care Med* **44**, 138-146 (2016).
- 466 45. Wrapp, D., *et al.* Cryo-EM structure of the 2019-nCoV spike in the prefusion conformation.
467 *Science* **367**, 1260-1263 (2020).
- 468 46. Hoffmann, M., *et al.* SARS-CoV-2 Cell Entry Depends on ACE2 and TMPRSS2 and Is Blocked
469 by a Clinically Proven Protease Inhibitor. *Cell* **181**, 271-280 e278 (2020).
- 470 47. Guillaume, V., *et al.* Nipah virus: vaccination and passive protection studies in a hamster model.
471 *J Virol* **78**, 834-840 (2004).
- 472 48. Mathieu, C., *et al.* Nipah virus uses leukocytes for efficient dissemination within a host. *J Virol*
473 **85**, 7863-7871 (2011).
- 474 49. Hartman, H., Wang, Y., Schroeder, H.W., Jr. & Cui, X. Absorbance summation: A novel
475 approach for analyzing high-throughput ELISA data in the absence of a standard. *PLoS One* **13**,
476 e0198528 (2018).
- 477 50. Pessi, A., *et al.* A general strategy to endow natural fusion-protein-derived peptides with potent
478 antiviral activity. *PLoS One* **7**, e36833 (2012).
- 479 51. Xia, S., *et al.* Fusion mechanism of 2019-nCoV and fusion inhibitors targeting HR1 domain in
480 spike protein. *Cell Mol Immunol* **17**, 765-767 (2020).
- 481

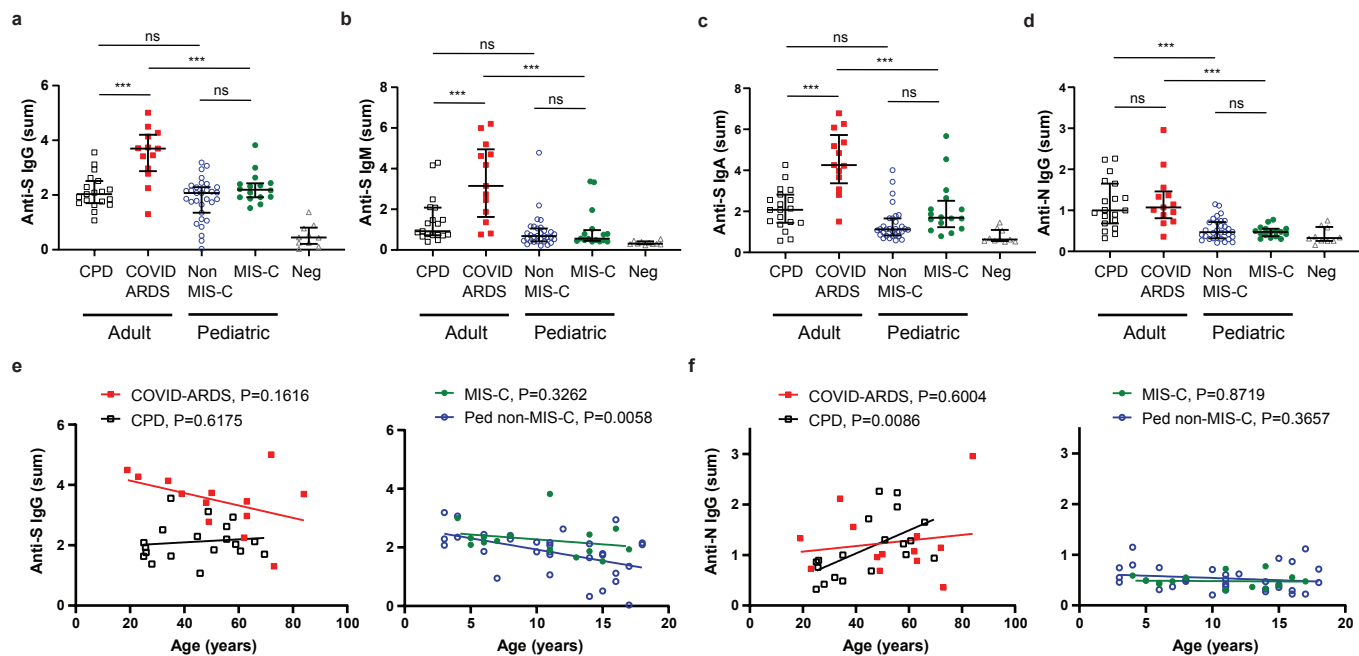


Figure 2

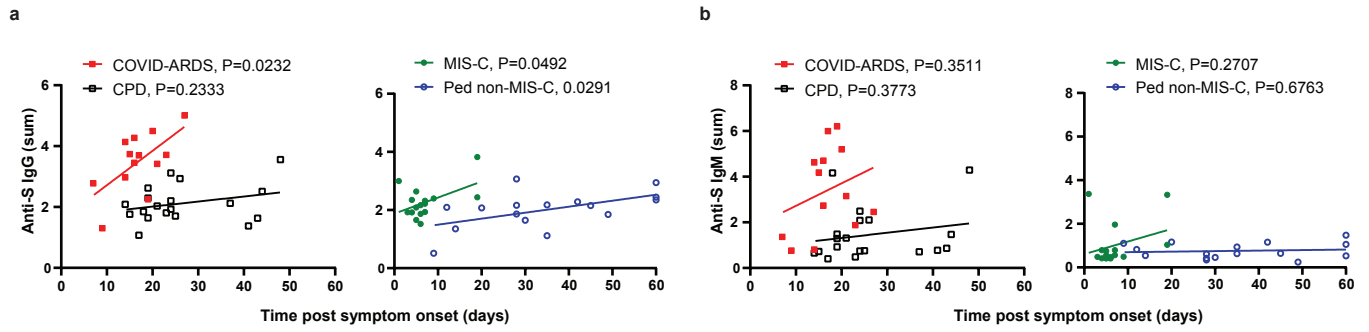


Figure 3

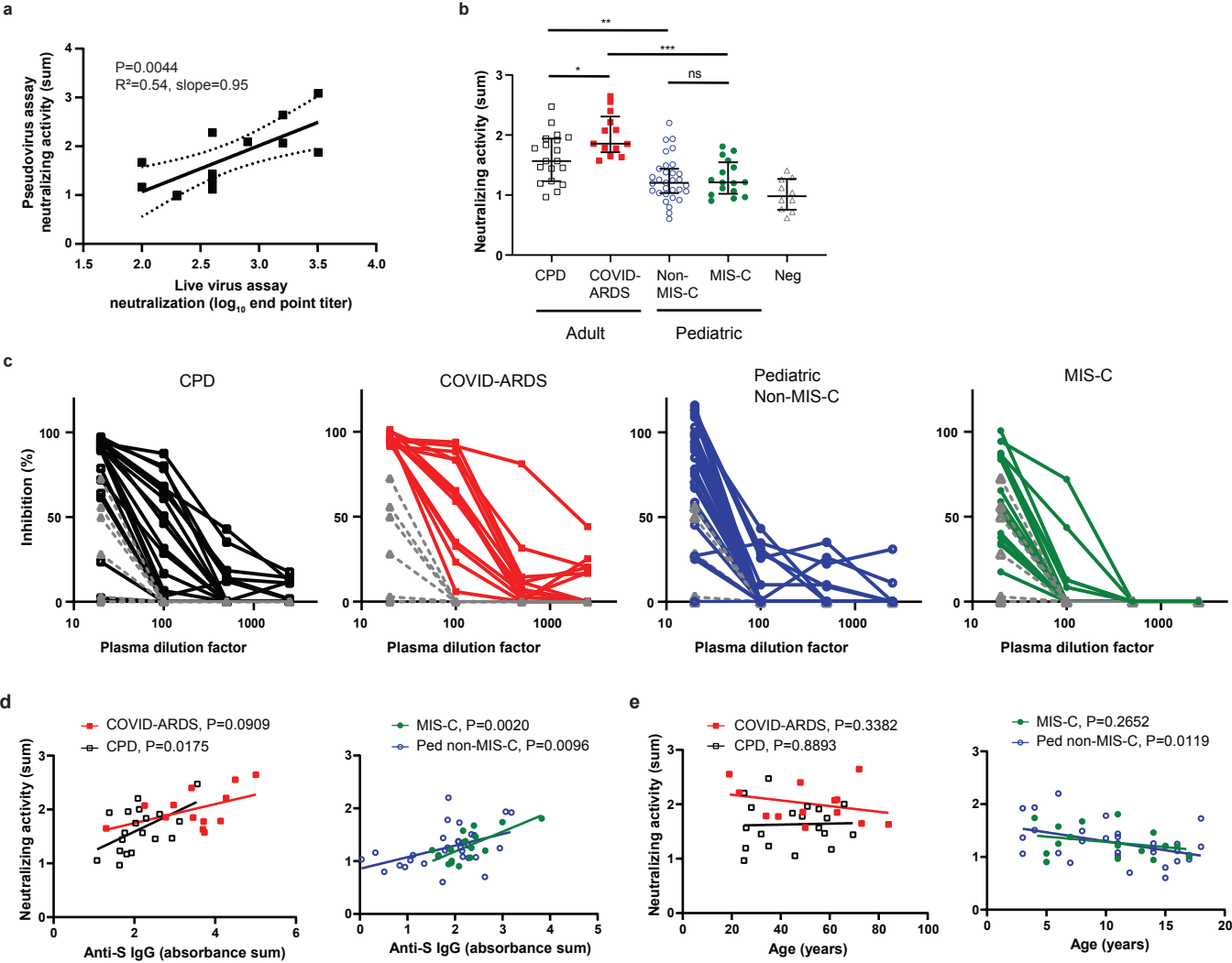
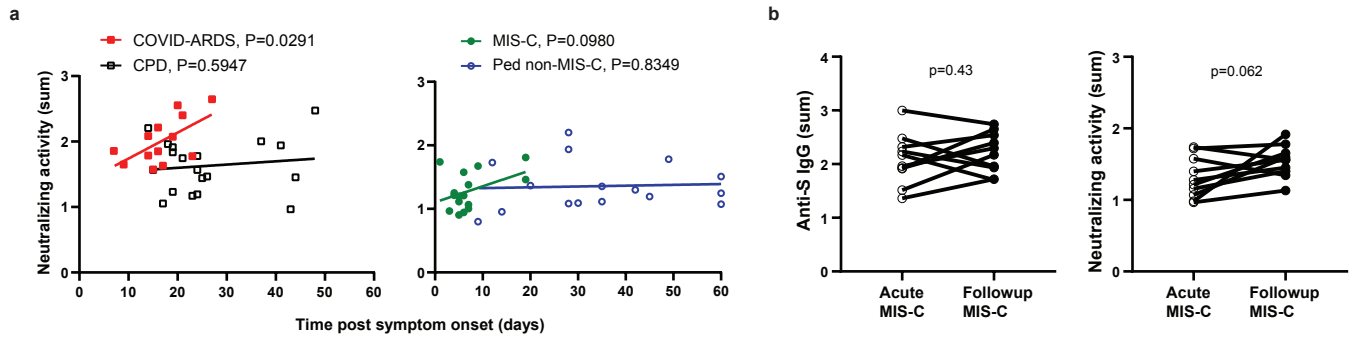


Figure 4



Extended data figure 1

